

Effects of cycling on the pseudoelastic properties of CuAlMnNi & TiNi based pseudoelastic alloys

N. Shajil, D. Das and L. Chandrasekaran*

Department of Applied Mechanics, Indian Institute of Technology Madras, Chennai-600 036.

ABSTRACT

The deformation responses of a Cu-Al-Mn-Ni alloy and that of a commercially available Ti-Ni wire, both pseudoelastic at room temperature, have been studied under cyclic loading-unloading conditions at fixed maximum stress levels corresponding to strains of 5, 4, 3 and 2 % respectively in the case of Cu-Al-Mn-Ni alloy and at a maximum stress level corresponding to 7.5 % strain in the case of the Ti-Ni alloy wire and compared with results reported on pseudoelastic Cu-Al-Be alloys. The characteristics of the pseudoelastic stress-strain curves of the Cu-Al-Mn-Ni alloys which change their shape drastically on cycling are very different from that of the Ti-Ni alloy. The area enclosed by the stress strain curves denoting energy dissipation also decreases sharply in the initial cycles but both shape and magnitude of energy dissipation tend to stabilize somewhat as cycling proceeds. From the point of view of energy dissipation capacity and the number of cycles to failure Cu-Al-Mn-Ni alloys seem to perform much better than Cu-Al-Be alloys thus giving rise to the possibility that they are a better choice than Cu-Al-Be alloys for low temperature damping applications where Ti-Ni alloys may not be suitable. The performance of the Ti-Ni alloy wire in terms of energy dissipation capacity, stability of shape and endurance however is orders of magnitude superior to that of the Cu-Al-Mn-Ni alloy.

1. INTRODUCTION

It is well known that the group of Titanium-Nickel and Cu-Al based materials known as shape memory alloys (SMAs) exhibit a property called pseudoelasticity (Wayman and Duerig, 1990). In the pseudoelastic condition Ti-Ni based SMAs can undergo large nonlinear deformations (~8%) under loading that can be recovered on subsequent unloading. This ability of the material to exhibit large recoverable strains is attributed to a mechanism called “stress induced martensite transformation”. A typical stress-strain plot obtained on a pseudoelastic Ti-Ni alloy in a complete loading cycle is shown in Figure 1. It is seen that the threshold stress values at the apparent yield point associated with the onset of stress induced transformation during loading and its reversal during unloading are not the same, causing a large hysteresis in the response curve. The presence of such a hysteresis indicates that a significant dissipation of energy takes place during such a loading-unloading process leading to the expectation that a pseudoelastic alloy could function as an effective damping material for incorporation in structures prone to seismic vibrations.

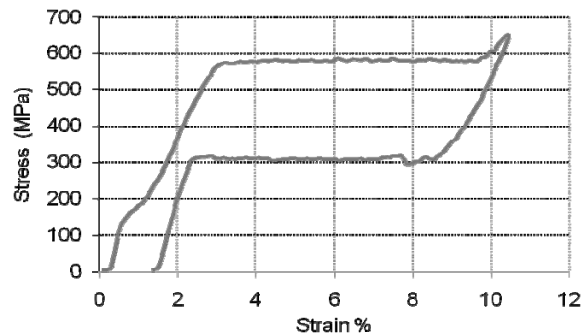


Figure 1 A Typical Stress-Strain Plot Obtained on a Superelastic NiTi Wire

Several articles have appeared in the literature describing the attempts to use Ti-Ni alloy based pseudoelastic alloys as reinforcements in such seismic damage-prone structures (Andrawes and Des Roches, 2005; Wilde, et al., 2000; Dolce, et al., 2007; Liu, et al., 2007; Choi, et al., 2005). Cu-Zn-Al based pseudoelastic alloys have not been seriously considered for such investigations in view of the fact that the degree of pseudoelasticity associated with them is not as high as that of Ti-Ni based pseudoelastic (PE) alloys. They are also prone to stress corrosion cracking, have low

* Email: l.chandra6@hotmail.com

strength, short fatigue life and are not amenable to manufacture of wires of diameter less than 1 mm. However, some investigations have been carried out on a rather less well-known Cu-Al-Be shape memory alloy for its possible use as a passive damping device for seismic response control of civil engineering structures (Casciati and Faravelli, 2004; Cerda, et al., 2006; Isalgue, et al., 2006).

Results from a very recent study on the mechanical properties of a pseudo elastic Cu-Al-Be wire indicate that it could be used in a re-centering damping device at temperatures lower than -50°C (Zhang, et al., 2008) where Ti-Ni based pseudoelastic alloys may not be suitable. Recently, a series of articles have appeared in the literature claiming that a new group of Cu-Al-Mn based alloys with higher degrees of pseudoelastic strains; better strength, ductility and higher fatigue life have been manufactured and shown to have better pseudoelastic properties than the conventional Cu-based SMAs (Omori, et al., 2002.; Sutou, et al., 2004.; Koeda, et al., 2005; Sutou, et al., 2005; Sutou, et al., 2006). It appears that they have the potential to be used as possible damping reinforcements in vibrating structures along with or in place of Ti-Ni alloys.

In view of this, the present study has been undertaken to investigate the pseudoelastic behaviour of a few chosen compositions from the Cu-Al-Mn based group of pseudoelastic alloys to evaluate their performance and compare it with that of Cu-Al-Be and Ti-Ni alloys. The results obtained on one of the Cu-Al-Mn based alloys subjected to cyclic loading at various degrees of strain in the range 2 to 5% are presented along with cyclic loading results obtained on a commercially available pseudoelastic Ti-Ni wire. From the results it is observed that while the Cu-Al-Mn based alloys do indeed show significantly larger pseudoelastic strain and better energy dissipation behaviour over a considerably larger number of cycles as compared to the Cu-Al-Be alloys, they do not however match the magnitude of pseudo elastic strain and number of cycles attainable in Ti-Ni alloy wires. In this paper, pertinent details regarding the preparation of pseudoelastic Cu-Al-Mn alloy and Ti-Ni wire specimens for cycling tests are described in section 2, followed by a description of the cycling test apparatus used in section 3. Experimental procedure and test results are summarized in section 4. Results are discussed in section 5 and conclusions drawn in section 6.

2. MATERIAL CHOICE-PREPARATION AND CHARACTERISTICS

Three Cu-Al-Mn based alloys and one Ti-Ni alloy were selected for investigation.

1. Cu-Al-Mn-Based Alloys

The selected alloy compositions for this particular study and their martensitic transformation temperatures in the appropriately heat treated condition are shown in Table 1 below.

Table 1. Composition of Cu-Al-Mn based alloys taken up for study

Alloy Code	Composition in (at %)							$M_s(^{\circ}\text{C})$	$A_f(^{\circ}\text{C})$
	Cu	Al	Mn	Ni	Co	Si	B		
#7(3)	71.54	16.66	9.80	2.0	-	-	-	-62	-43
#6(2)	72.13	16.92	10.45	-	0.5	-	-	-60	-41
#5(1)	71.28	16.95	11.47	-	-	0.1	0.2	-19	2

The above alloys were cast, rolled and supplied in the form of 200 mm x 40 mm x 20 mm rectangular ingots by Y Sutou of Tohoku University Sendai, Japan. All the ingots were hot rolled at 800°C down to 5.5 mm thick strips in a large rolling mill at QinetiQ Ltd, UK. These were then given an anneal at 600°C for 30 minutes to obtain an ($\alpha + \beta$) microstructure to facilitate the evolution of a favourable texture during further cold rolling. Further cold rolling was carried out at 20% reduction steps, with intermediate annealing at 600°C for 30 minutes after every reduction step to realize strips of thickness ~ 2.0 mm. Strips of Alloy # 7(3) were chosen for the first series of experiments. Non standard specimens of rectangular cross sectional area between 1.3 and 2.6 mm² and of length around 70 mm were cut along the rolling direction of the strips and given a $930^{\circ}\text{C} / 8$ minutes / water quench + $200^{\circ}\text{C} / 15$ minutes / air cool heat treatment to ensure that their stabilized transformation temperatures M_s (martensite start temperature) and A_f (Austenite finish temperature) were -62°C and -43°C respectively at zero stress conditions. Figure 2 shows the microstructure of the alloy after the heat treatment. It is clear from Figure 2 that the alloy is made up of single β phase grains varying in size from 0.2 mm to 2.5 mm, satisfying the essential requirement for the presence of pseudo elastic behaviour in Cu-Al-Mn based alloys, namely that it should consist only of single β phase grains. The measured M_s & A_f temperatures confirm the expectation that this alloy would show pseudoelastic behaviour at room temperature and below down to -43°C .

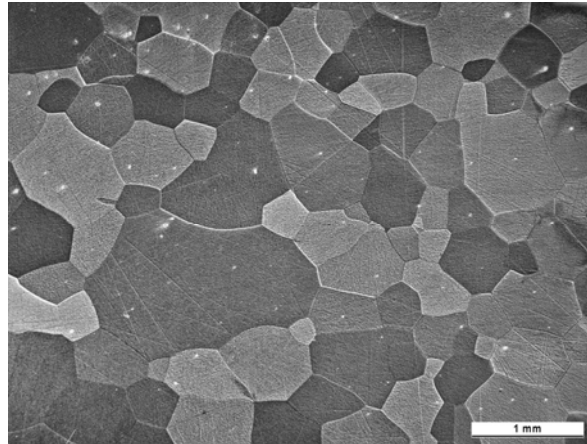


Figure 2 Microstructure of Cu-Al-Mn-Ni Alloy # 7(3) After 930°C/8 Minutes/Water Quenched + 200°C/15 Minutes/Air-Cooled Treatment

2. TiNi Alloy

The TiNi alloy chosen for the present experiments was commercially available in the form of processed pseudoelastic wire of diameter 213 microns from Memory-Metalle, Basel, Germany designated as Alloy N wire. This wire was expected to have an A_s temperature below 0°C and exhibited pseudoelastic behavior at a specific stress value at room temperature (~30°C) as shown in Figure 1 Specimens cut from this wire were subjected to cyclic loading experiments directly without any further processing

3. EXPERIMENTAL APPARATUS



Figure 3 Experimental Set-up for Cyclic Loading Experiments on SMA Wires

The experimental apparatus used for cyclic loading-unloading experiments consists of a specially constructed horizontal bench tensile testing machine somewhat akin to the Hounsfield tensile testing machine in design. It consists of a horizontal rigid rectangular metallic base frame with a cross-head housing a load cell and adjustable grips (to act as specimen holders) fitted to the immovable short arm rigidly fixed on one side of the rectangular frame. A movable arm parallel to the fixed arm, fitted with another cross-head with similar specimen holder grips and whose speed of movement can be controlled by a computer operated stepper motor that provides a mechanism for applying extension to the specimen. An LVDT sensor attached to the movable cross head is used for measuring the extension of the specimen during testing. The measurements of the load and the length change experienced by the specimen during the experiment are continuously logged on to a computer using LABVIEW software which

allows one to post- process the data in different formats. The experimental set-up described above and used in this study is shown in Figure 3.

1. Cu-Al-Mn-Ni # 7(3) Alloys

The aim of the experiments was to subject test specimens to stress cycling at a constant stress commensurate with a chosen initial pseudoelastic strain value and follow the change in the nature of the resulting stress-strain curves with cycling until fracture. A total of six specimens were subjected to such stress cycling experiments. The cyclic loading experiments conducted on specimen 1 were exploratory in nature, carried out with the main aim of semi-quantitatively estimating 1) the degree of pseudoelasticity sustainable over a number of cycles in this alloy, 2) the energy dissipation efficiency, 3) the tendency for accumulation of remnant plastic deformation and 4) the cyclic loading response on progressively increasing the strain reached in a cycle up to a limit estimated as the safe limit for pseudoelastic response. Figures. 4 to 8 pertain to the data related to the above characteristics obtained on specimen 1. Table 2 below gives the dimensions, maximum strain and the number of cycles before fracture of non- standard specimens subjected to cyclic loading experiments at a strain rate in the interval $3-5 \times 10^{-4}$ /sec. All the tests were conducted at 29°C.

4. EXPERIMENTAL PROCEDURE AND RESULTS

First three specimens (specimens 1,2 & 3) were subjected to a maximum stress corresponding to a pseudoelastic strain limit of ~ 5% in the initial cycle while the rest (specimens 3 to 6) were subjected to maximum stresses corresponding to pseudoelastic strains of 4, 3 & 2% respectively in the initial cycle. Experiments conducted on specimen 2 were more specifically oriented towards the precise measurement of change in the magnitude of pseudoelastic strain, dissipation energy and the remnant plastic deformation as a function of cycling up to a fixed value of stress commensurate with a chosen value of pseudoelastic strain (~5%) in the first cycle. The effect of reducing the maximum stress after the first 150 cycles till the 250th cycle was also recorded and further cycling resumed at the original higher value of stress till the specimen fractured. Figures. 9 to 13 pertain to data related to the above mentioned variations in test conditions imposed on specimen 2.

Table 2. Details of Alloy # 7(3) Specimens Subjected to Cycling Experiments

Specimen ID	Cross Section Area (mm ²)	Gauge Length (mm)	Max.Strain @ Start (%)	No. of Cycles to Fracture
# 7(3)-1	2.64	72.0	5	100(still intact)
# 7(3)-2	1.31	69.06	5	326
# 7(3)-3	1.30	68.92	5	245
# 7(3)-4	1.37	65.65	4	959
# 7(3)-5	1.76	66.49	3	513
# 7(3)-6	1.22	55.54	2	1188

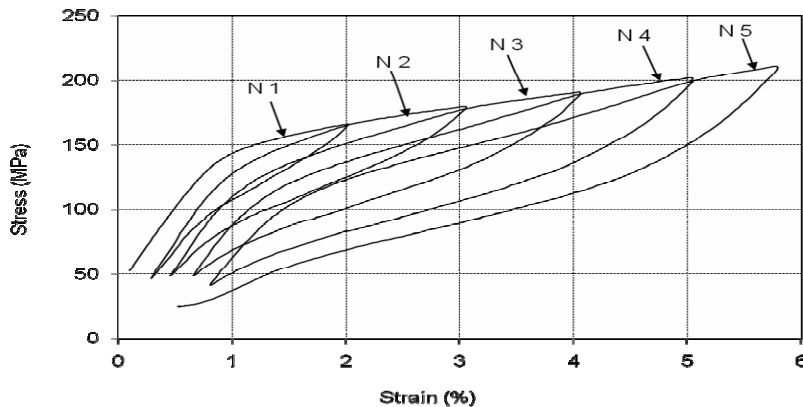


Figure 4: Deformation Behaviour of Virgin Specimen (Specimen 1)–First Few Cycles.

Notice that in the Initial Cycles there is a Significant Accumulation of Residual Plastic Strain. Also, the Shape of the Pseudoelastic Curve is Quite Different from the one that is Observed for Conventional TiNi as Shown in Figure 1 in that there is no Distinct Plateau in the Stress-Strain Curve Corresponding to the Onset of Stress Induced Martensite.

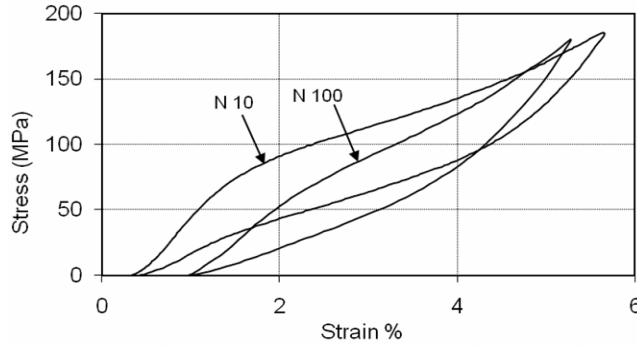


Figure 5: Deformation Behaviour of Specimen 1(5% PE Strain) between Cycles 10 and 100. Notice that the Shape of the Loop has changed from the 10th Cycle to the 100th Cycle

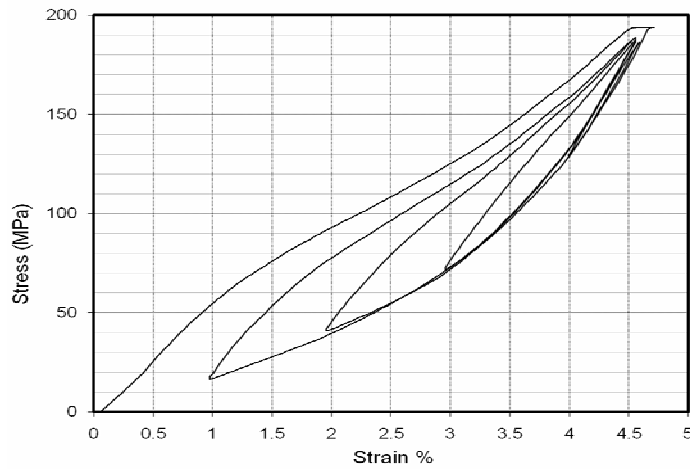


Figure 6: Loading to a Fixed Large Strain in the Loading Part of the Cycle and Progressive Partial Unloading to Smaller Strain Values (Specimen 1– Loading After 100 Cycles)

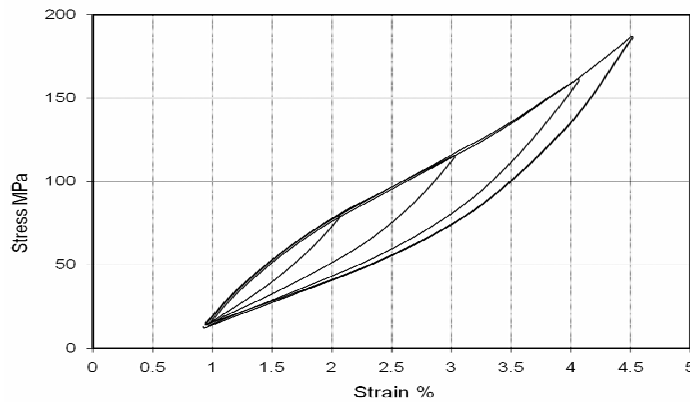


Figure 7: First Cycle Loading to a Small Value of Strain and Subsequent Loading Cycles with Increasing Strain Limits on Loading (Specimen 1 – Loading After 105 Cycles)

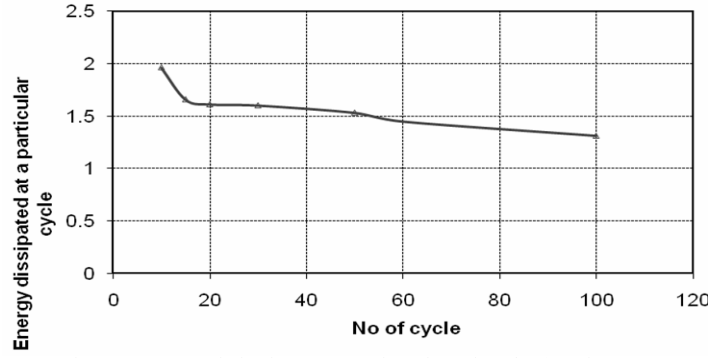


Figure 8: Energy Dissipation as a Function of N° of Cycles (Specimen 1)

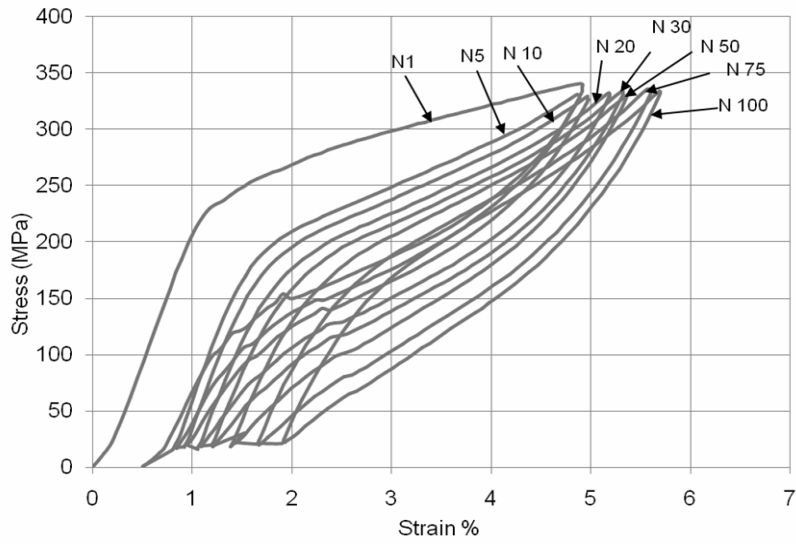


Figure 9: Deformation Behaviour of Specimen 2(5% PE Strain) between Cycles 1 and 100

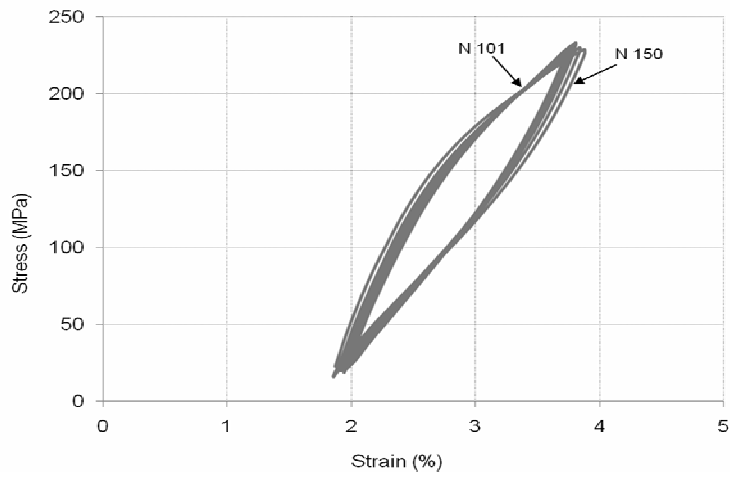


Figure 10: Deformation Behaviour of Specimen 2 between Cycles 101 and 150.

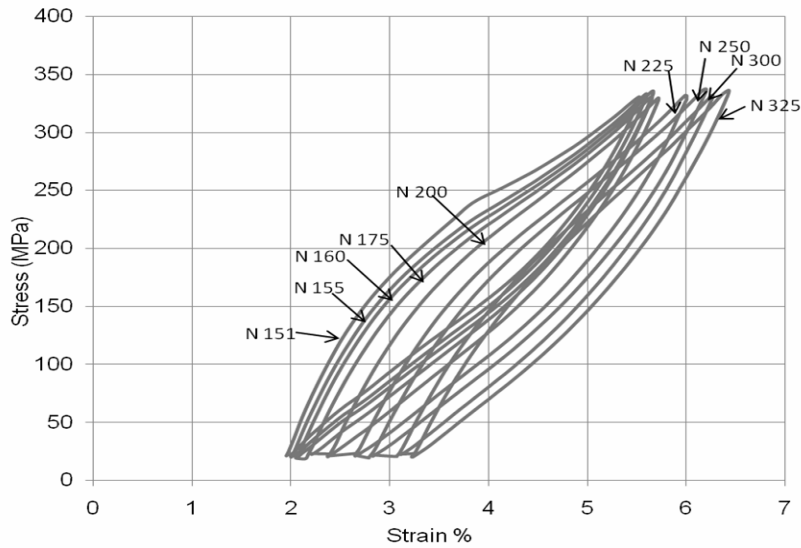


Figure 11: Deformation Behaviour of Specimen 2(5% SE Strain) between Cycles 151 and 325

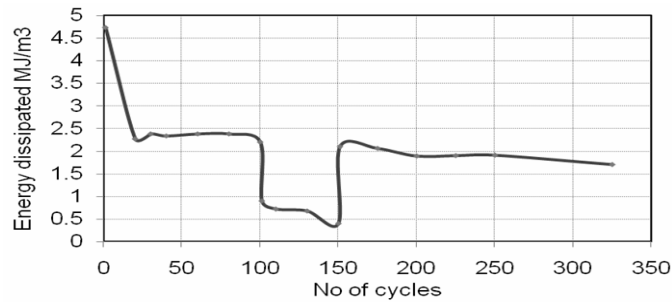


Figure 12: Energy Dissipated as a Function of N° of Cycles (Specimen 2)

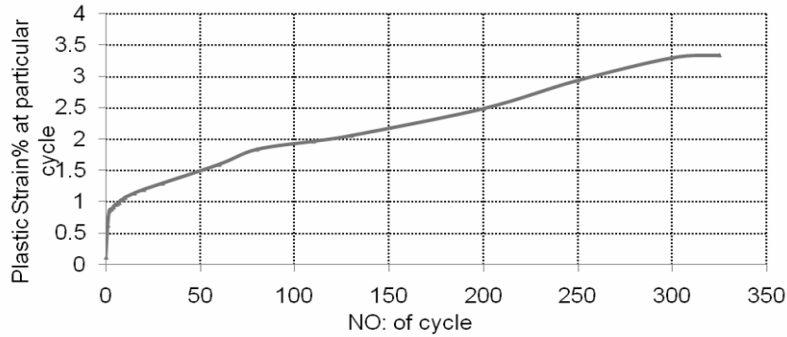


Figure 13: Remnant Plastic Strain as a Function of N° of Cycles (Specimen 2)

Experiments conducted on specimen 3 were similar to those conducted on specimen 2 except that the cycling was carried out at a single stress value chosen after the first cycle, till the specimen fractured. Figures. 14 to 16 pertain to the data obtained on specimen 3. Experiments conducted on specimens 4 to 6 were aimed at generating similar cycling test data at decreasing values of maximum starting stress corresponding to strains of 4, 3 and 2% respectively. Figures. 17 to 19 show the stress-strain curves obtained for each of these specimens at various intervals of cycling.

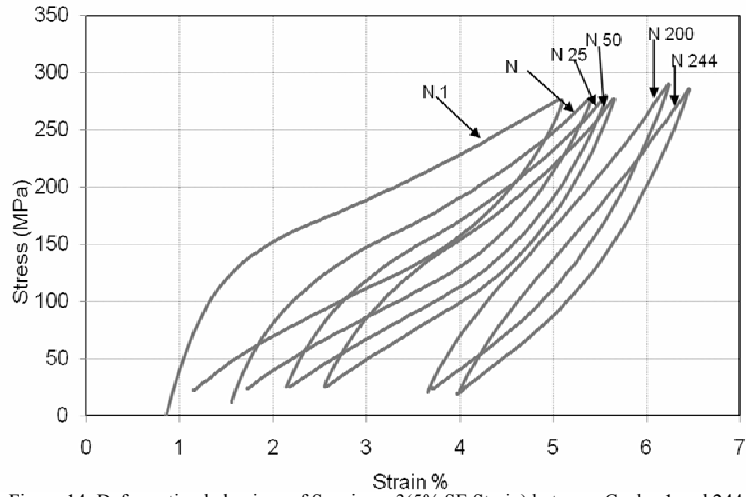


Figure 14: Deformation behaviour of Specimen 3(5% SE Strain) between Cycles 1 and 244

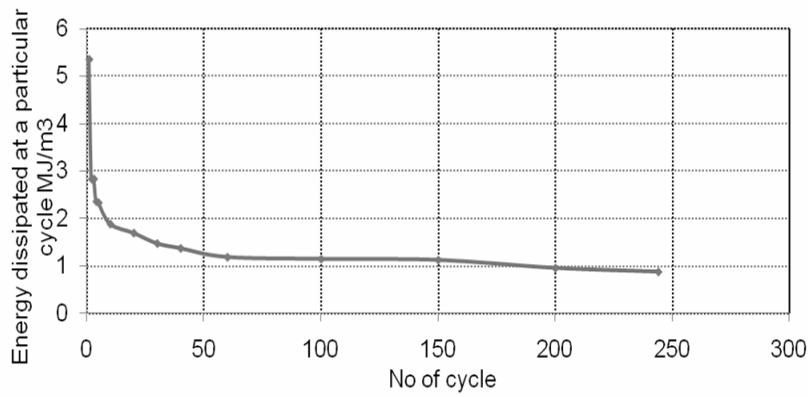


Figure 15: Energy Dissipated as a Function of N° of Cycles (Specimen 3)

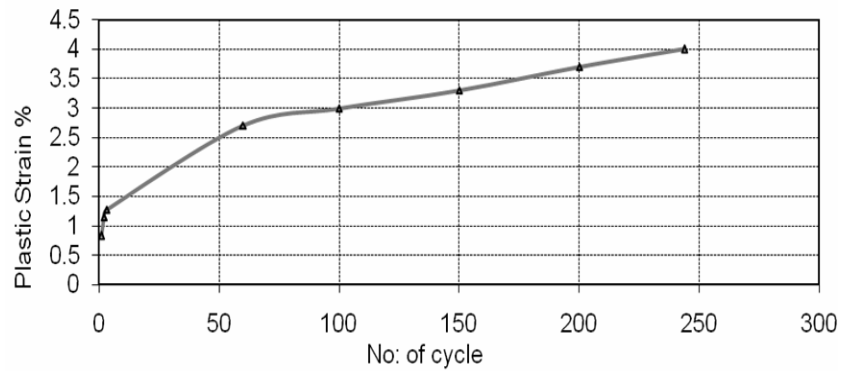


Figure 16: Remnant Plastic Strain as a Function of N° of Cycles (Specimen 3)

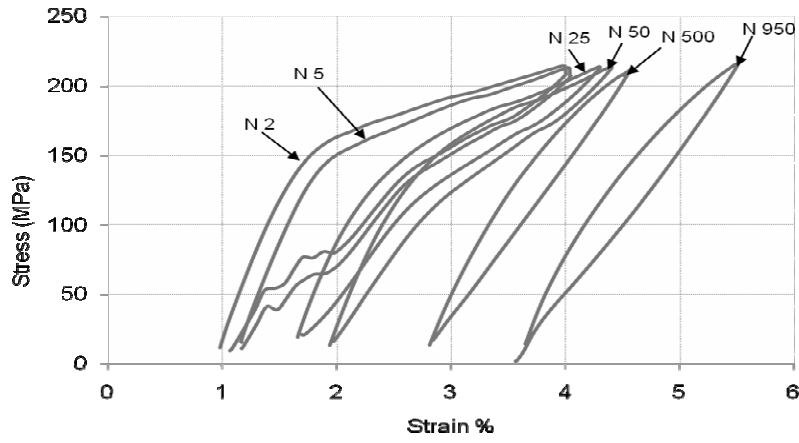


Figure 17: Deformation behaviour of Specimen 4(4% PE Strain) between Cycles 1 and 950

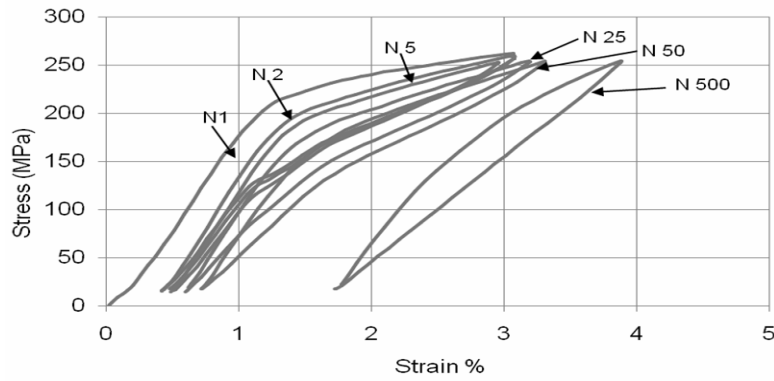


Figure 18: Deformation Behaviour of Specimen 5(3% SE Strain) between Cycles 1 and 500

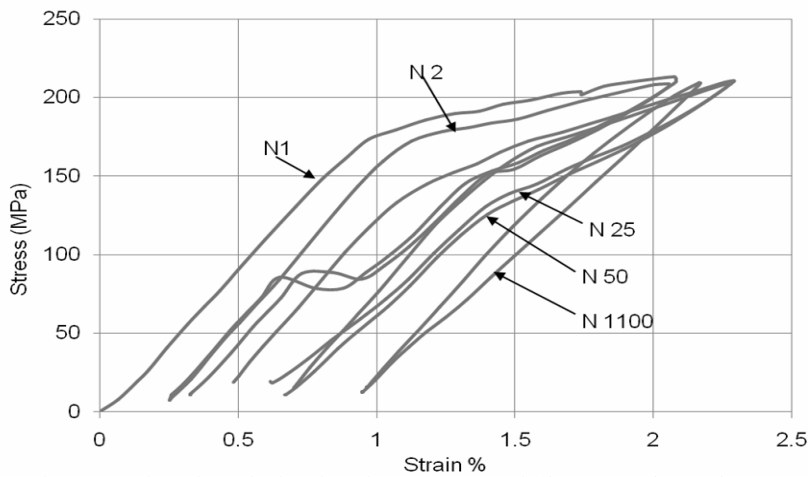


Figure 19: Deformation Behavior of Specimen 6(2% PE Strain) between Cycles 1 and 1100

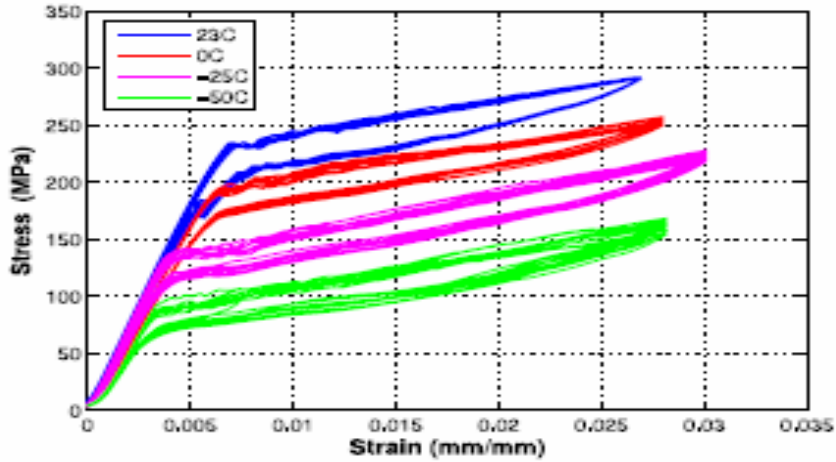


Figure 20: Loading Curves Obtained on Cu-Al-Be Alloys (from Ref. 10) Batch 1, $\epsilon = 0.0012 \text{ s}^{-1}$

2. TiNi Alloy Wire

Cyclic loading-unloading experiments were performed on 213 micron ϕ wire of this alloy (designated as Alloy N) at a temperature $T = 29^\circ\text{C}$. Cycling test was conducted such that the maximum and minimum stresses attained during loading and unloading respectively were the same in all cycles. Maximum stress limit reached in every cycle was fixed at a value (575 MPa) corresponding to a strain just above the second inflexion in the first cycle on the loading curve. Minimum stress limit was fixed at 50 MPa. Maximum number of cycles was limited to 330 because of time constraints. The specimen remained intact after 330 cycles. Figures. 21 to 26 pertain to the data obtained on Alloy N wire.

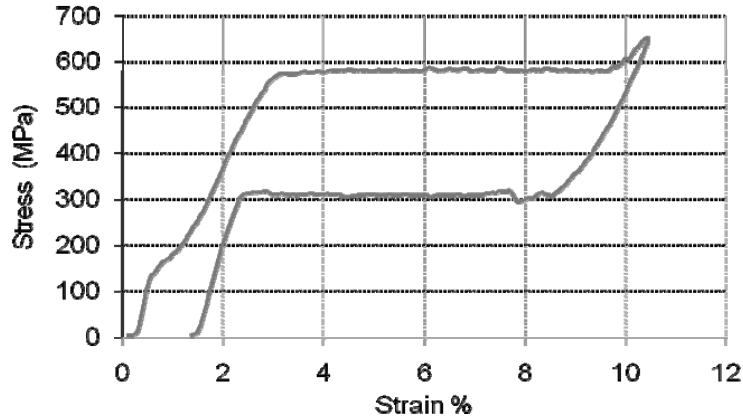


Figure 21: Deformation Behaviour of TiNi Alloy N Wire – Cycle 1

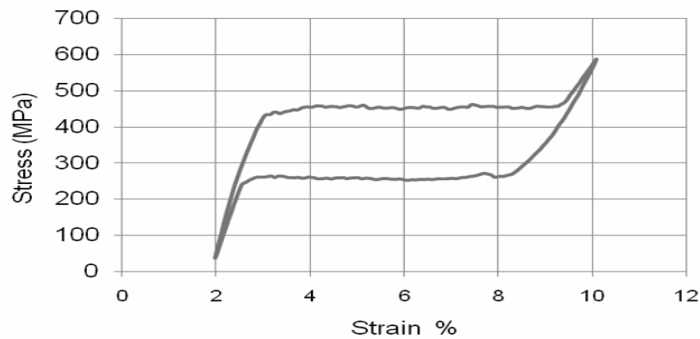


Figure 22: Deformation Behaviour of TiNi Alloy N Wire – Cycle 100

Note: The residual plastic strain was observed to have stabilized by the 100th cycle and in the subsequent cycles the plastic strain value remained the same on reaching zero stress on unloading. Hence the shift to zero on the strain axis in figure 23.

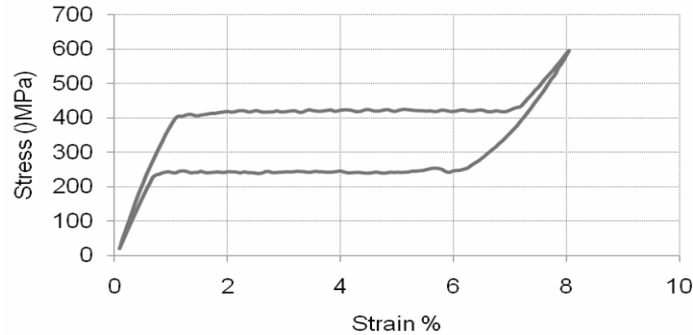


Figure 23: Deformation behaviour of TiNi Alloy N Wire – Cycle 320)

5. DISCUSSION

1. CuAlMnNi Alloys

It is evident from an examination of Figure 4 that Cu-Al-Mn-Ni alloy exhibits pseudoelastic behaviour and that initial pseudoelastic strains of the order of 5% can be realized in this alloy. It is also seen that in the initial cycles there is a significant accumulation of residual plastic strain. The most significant observations on the nature of pseudoelastic response in these alloys are as follow:

1) The shape of the pseudoelastic curve is quite different from the one that is observed in the case of conventional Ti-Ni and Cu-Al based alloys. This may have a significant bearing on how modeling of pseudoelastic behaviour should be approached in such alloys. There is no distinct plateau in the stress-strain curve corresponding to the onset of stress induced martensite, even though there is a distinct change of slope seen in the initial cycles.

2) The stress corresponding to this slope change decreases rapidly, when cycling is carried out in such a way that the maximum stress on the loading part of the cycle is fixed at a constant value corresponding to the stress that produced ~5% strain in the first cycle.

3) The shape of the loop also changes with cycling and after about 10 cycles the loop shapes are as shown in Figure 5. This change in shape would again be expected to influence the criteria to be adopted in modeling. It is further seen from Figures. 6 & 7 that even after a substantial number of cycles the near lenticular shape of the loops is maintained.

4) The locus of stress values corresponding to different strains reached during unloading lies on the same unloading curve in Figure 6. Similarly the locus of stress values reached during loading to different strains lies on the same loading curve in Figure 7.

5) It can be seen that in the first few cycles there is a very drastic change in the loop area i.e. in the dissipation energy; however, after about 20 cycles the rate of change in the loop shape and loop area is reduced significantly. The rate of decrease of dissipation energy comes down after about 20 cycles as can be seen in Figure 8. At the end of 100 cycles the energy dissipated per cycle is $\sim 1.5 \text{ MJ/m}^3$.

The observations made above on the pseudoelastic response of specimen 1 are confirmed by the results obtained on specimen 2. From Figure 9 it is clear that the specimen shows $\sim 5\%$ pseudoelastic strain in the first cycle which decreases drastically in the initial cycles leading to similar shape and area changes associated with the loop. From Figure 12 it is seen that in the first 100 cycles, where the maximum stress reached corresponds to the stress reached at $\sim 5\%$ in the first cycle, the energy dissipated in the 100th cycle is $\sim 1.9 \text{ MJ/m}^3/\text{cycle}$ marginally larger than that observed in case of specimen 1. The accumulated plastic strain is $\sim 2\%$ at the end of 100 cycles as is seen from Figure 13.

The effect of reducing the maximum stress reached during loading such that the resulting strain was $\sim 2\%$ instead of $\sim 5\%$ on the shape of the loop in the subsequent 50 cycles is shown in Figure 10. It is seen from Figures. 12 & 13 that the dissipation energy and the total remnant plastic deformation at the end of 150 cycles are $\sim 0.4 \text{ MJ/m}^3/\text{cycle}$ and $\sim 2.2\%$ respectively. It is interesting to note that the rate of reduction in the magnitude of energy dissipation, as seen from the slope of the line in Figure 12 is not significantly altered.

Resumption of cycling at the original higher stress value seems to have no noticeable effect on the shape of the curve seen in the 100th cycle (Figure 11). The rate of reduction in the magnitude of energy dissipation, indicated by the slope of the line in Figure 12 also seems to be almost the same as observed in the 100th cycle. The rate of plastic

deformation accumulation also behaves in the same way (Figure 13). When the specimen failed on the 325th cycle the total plastic strain that had accumulated was around 3.8% and the energy dissipation stood at ~ 1.7 MJ/m³/cycle.

Table 3. Energy Dissipated Vs No. of Cycles

Specimen ID	Energy dissipation at cycle number (MJ / m ³)											
	1	2	5	10	20	50	100	200	300	400	500	1000
#7(3)-1				1.96	1.61	1.53	1.31					
#7(3)-2	4.73				2.27			1.89				
#7(3)-3	5.36	2.83	2.33	1.88	1.69	...	1.14	0.95				
#7(3)-4	1.36	1.19	1.13	...	0.65	0.63	0.58	0.50	0.49	0.42	
#7(3)-5	1.35	0.74	0.59	0.59	0.69	0.76	...	0.63	0.7	0.69	
#7(3)-6	0.84	0.53	..	0.67	0.58	0.27		0.24	0.19	0.17	0.16	0.18

Results obtained on specimen 3 shown in Figures. 14, 15 & 16 confirm the trends observed in the pseudoelastic response of the first two specimens, as regards the shape of the loop, the energy dissipation with cycling and the accumulation of plastic deformation with cycling. There is however, a difference in the magnitude of energy dissipated and also in the magnitude of plastic strain with cycling. One of the reasons for this difference in magnitude of the energy dissipated and the plastic strain accumulation could be the non-uniform nature of the grain size in the specimens. It can be seen from Figure 2 that the grain size varies from 0.2 mm to 2.5 mm in the alloy after the appropriate heat treatment to confer pseudoelastic behaviour. Figures. 17 to 19 shows the cyclic stress- strain curves corresponding to starting pseudoelastic strains of 4, 3 and 2% respectively and the progressive change in the nature of the curves as a function of cycles. It is evident from these Figures. that the rate of reduction in the area enclosed by the curves is very high in the first few cycles but attains an almost steady state value after about ~ 20 cycles. In Table 3 below the dissipation energy values calculated from the enclosed area for each specimen is tabulated as a function of cycles for all the specimens tested. It is obvious that reducing the maximum PE strain to lower values increases the cycling life of the specimen quite considerably. It is also interesting to note from Table 4 that, in spite of a gradual accumulation of plastic strain with cycling, the magnitude of pseudoelastic strain associated with the specimens is surprisingly still quite significant even at cycles quite near the break in all the specimens tested.

Table 4. Comparison of Pseudoelastic and Remnant Plastic Strains @ Start of Cycling and Near Break

Specimen ID	Max strain at initial cycle % (X1)	Plastic strain @initial cycle% (Y1)	Super elastic strain % @ start (X1-Y1)	Max strain of cycle near break % (X2)	Plastic strain of cycle near break (Y2)	Super elastic strain% @ near break (X2-Y2)
# 7(3)-1	5	0.28	4.72	5.27	1.01 intact after 100 cycles	4.26
# 7(3)-2	5	0.63	4.37	6.39	3.22	3.17
# 7(3)-3	5	0.83	4.17	6.45	3.94	2.51
# 7(3)-4	4	1.16	2.84	5.6	3.73	1.87
# 7(3)-5	3.0	0.4	2.6	3.94	1.77	2.17
# 7(3)-6	2.0	0.25	1.75	2.25	1.24	1.01

2. Comparison with Cu-Al-Be Alloy Behavior

Zhang, et al., (2008) have carried out investigations on Cu-Al-Be alloys and their observations are as follow. The Cu-Al-Be alloy chosen had A_s and A_f equal to -105°C and -65°C respectively in the heat treated single β phase state and it showed pseudoelastic behaviour in the range -80°C to $+100^\circ\text{C}$. The wires of these alloys showed pseudoelastic

behaviour, but required a few cycles initially to exhibit a steady state pseudoelastic response. Specimens stabilized in this manner were cycled at different test temperatures to a maximum limit of 3% strain. The maximum number of cycles the specimens could withstand before fracture seemed to depend on temperature. It varied from 90 cycles at 23°C to 170 cycles at -50°C. Typical pseudoelastic response curves obtained at a strain rate of 0.0012s^{-1} at different temperatures are reproduced from their paper in Figure 20. The values of energy dissipation associated with the pseudoelastic loops at 23 °C, 0°C, -25 °C and -50°C calculated from the area enclosed by the loops are 0.47, 0.42, 0.50, 0.39 MJ/m³/cycle respectively.

Comparing the results obtained on the Cu-Al-Mn-Ni alloy with the results obtained on Cu-Al-Be, it is very clear that from the point of view of energy dissipating ability that the Cu-Al-Mn-Ni alloy has an advantage over Cu-Al-Be alloys in that it can withstand large strains over a large number of cycles without fracture and dissipate similar magnitude of energy, if not larger, at lower strain values. The persistence of pseudoelastic behaviour in spite of the accumulation of plastic strain is also a significant advantage.

3. TiNi Alloy (Alloy N)

The most significant general observations that can be made on examining the loading unloading curves shown in Figures 21 to 26 are as follow:

- 1) The upper and lower plateaus are sharply defined and stay flat even after a large number of cycles.
- 2) The magnitude of energy dissipation, measured as the area under the curve, decreases with the number of cycles.
- 3) The threshold stress σ_{SIM} for inducing martensite also decreases with number of cycles.
- 4) The residual plastic strain increases at a fast rate in the initial cycles but tends to stabilize asymptotically in the later cycles
- 5) In spite of the increase in the residual plastic strain the pseudoelastic strain realized in each cycle with the increase in number of cycles remains almost constant at around ~7.5 %.

It is seen from Figures. 21 and 22 that after the first loading cycle there is a residual plastic strain of the order of ~ 1.5% which increases slowly to ~ 1.96% in 100 cycles and stays constant at that value till the end of 325 cycles. The reason for the buildup of plastic strain at a fast rate in the initial cycles could be due to the strain exceeding ~6%, thereby causing onset of slip in the matrix. With continued cycling at such high strains accumulation of plastic strain occurs resulting in work hardening of the matrix. The work hardened matrix prevents further plastic deformation leading to stabilization in the values of energy dissipated and in the value of σ_{SIM} (Miyazaki, 1990). From Figures. 23 & 24 it is seen that energy dissipation and σ_{SIM} follow the same trend namely, an initial fast rate of decrease with cycles and a much slower rate of decrease in later cycles. It is interesting to note that the plastic residual strain reaches a constant value of ~ 2% in less than 100 cycles in Figure 25. This residual deformation does not seem to seriously affect the rate of energy dissipation decrease with cycling. The steady state energy dissipation value is ~ 10 MJ/m³/cycle and the rate of energy dissipation reduction is 0.13 MJ/m³ /cycle after about ~ 80 cycles. A comparison of these results with results obtained by Miyazaki, et al., (1990) leads one to conclude that the magnitude of energy dissipation achieved in TiNi alloy in the present work is much larger. However such a comparison is not strictly justifiable because the strain limits reached in the present experiments were ~8% as compared to the 2% limit adopted by Miyazaki et al.

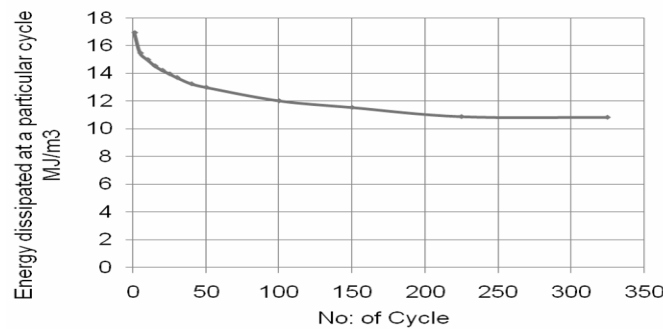


Figure 24: Energy Dissipation Vs No: of Cycles (Ti-Ni Alloy N)

It is also not known how comparable are the transformation temperatures of Alloy N wire and those investigated by Miyazaki. It is however quite obvious that the material used in the present case is much closer to an ideal pseudoelastic material than the one used by Miyazaki which does not show as flat a plateau as the material used in the present experiments. On the basis of these results it is inferred that the material used in the present experiments is superior to

the one used by Miyazaki, probably due to better processing techniques evolved over the years in achieving superior quality wires.

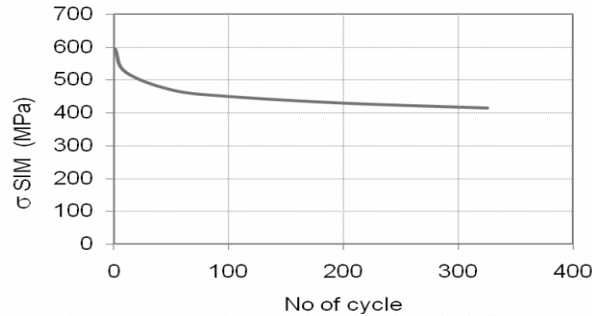


Figure 25: σ_{SIM} as a function of N° of Cycles (Ti-Ni alloy N)

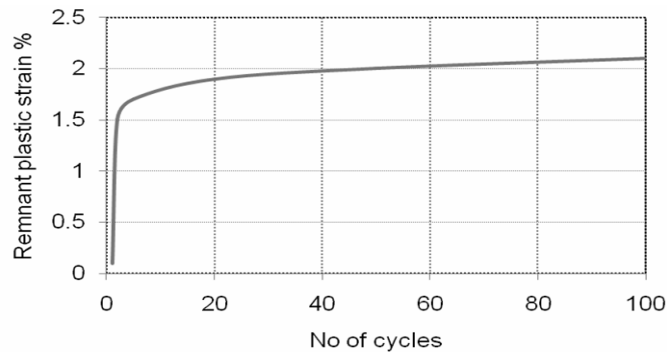


Figure 26: Residual plastic strain as a function of N° of Cycles (Ti-Ni alloy N)

4. Comparison of pseudoelastic behaviour of CuAlMnNi and TiNi alloys

It is clear from a comparison of the pseudoelastic loops of Cu-Al-Mn-Ni & Ti-Ni shown elsewhere that the pseudoelastic loop observed in the case of Cu-Al-Mn-Ni is quite different from that observed in Ti-Ni and Cu-Al-Be in the sense that the Cu-Al-Mn-Ni alloy does not exhibit a sharp change in the slope of the loading curve in the stabilized condition as it is seen in the case of Ti-Ni wire and the Cu-Al-Be wire. The shape of the loop also tends to evolve into a lenticular shape with cycling which seems to be the characteristic of this alloy. The steady state energy dissipation by this alloy at the largest strain amplitude of strain ($\sim 5\%$) is of the order of 1 to 1.7 MJ/m³/cycle while that of Ti-Ni is ~ 10 MJ/m³/cycle. The plastic strain accumulation tends to level off at $\sim 2\%$ in the Ti-Ni alloy in 100 cycles while it continues to increase, albeit at a slow rate, to 4% leading to eventual fracture in the case of the Cu-Al-Mn-Ni alloy.

6. CONCLUSIONS

1. A typical Cu-Al-Mn-Ni based pseudoelastic alloy has been shown to exhibit better pseudoelastic behaviour over a large number of cycles as compared to a conventional Cu-Al-Be alloy.
2. The shape of the pseudoelastic loop is quite different from those normally seen in conventional Ti-Ni & Cu-Al based PE alloys.
3. Dissipation energies of the order of 1 to 1.7 MJ/m³/cycle are realizable over a number of cycles (> 200) at large strain amplitudes in these alloys.
4. Ti-Ni (Alloy N) wire shows ideal pseudoelastic behaviour with well defined upper and plateaus that persist over a large number of cycles.
5. Dissipation energies of the order of 10 MJ/m³ / cycle are realized in these wires over a number of cycles.

REFERENCES

- Andrawes, B. and Des Roches, R. (2005). Unseating Prevention for Multiple Frame Bridges using Superelastic Devices, *Smart Mater. Struct.* Vol. **14**, pp. 60-67.
- Casciati, F. and Faravelli, L. (2004). Experimental Characterization of a Cu-based Shape Memory Alloy towards Its Exploitation in Passive Control Devices, *Jl. Physique IV* Vol. **115**, pp. 299-306.
- Cerda, M., Boroschek, R., Faras, G., Moroni, O. and Sarrazin, M. April (2006). Shaking Table Test of a Reduced – Scale Structure with Cu-based SMA Energy Dissipation Device, *Proc. 8th US National Conf. on Earthquake Eng.* (San Francisco, CA).
- Choi, E., Nam, T. H. and Cho, B. S. (2005). A New Concept of Isolation Bearings for Highway Steel Bridges using Shape Memory Alloys, *Can J. Civ. Eng.* Vol. **32**, pp. 957-967.
- Dolce, M., Cardone, D. and G. Palermo. (2007). Seismic Isolation of Bridges using Isolation Systems based on Flat Sliding Bearings, *Bull. Earthquake. Eng.* Vol. **5**, pp. 491-509.
- Isalgue, A., Lovey, F. C., Terriault, P., Martorell, F., Torra, R. M. and Torra, V. (2006). SMA for Dampers in Civil Engineering, *Mater. Trans.* Vol. **47**, pp. 682-690.
- Koeda, N., Omori, T., Sutou, Y., Suzuki, H., Wakita, M., Kainuma, R. and Ishida, K. (2005). Damping Properties of Ductile CuAlMn based Shape Memory Alloys, *Mat. Trans.* Vol. **46(1)**, pp. 118-122.
- Liu, M., Li, H., Song, G. and Ou, J. (2007). Investigation of Vibration Mitigation of Stay Cables Incorporated with Superelastic Shape Memory Alloy Dampers, *Smart. Mater. Struct.* Vol. **16**, pp. 2202-2213.
- Miyazaki, S. (1990). Engineering Aspects of Shape Memory Alloys edited by Duerig, T.W., et al; *Published by Butterworth- Heinemann*, London .pp 394-413.
- Omori, T., Kainuma, R., Ono, N. and Ishida, K. (2002). Enhancement of Superelasticity in CuAlMnNi Shape Memory Alloys by Texture Control. Y. Sutou, *Met & Mat. Trans.A.* Vol. **33A**, pp.2817-2824.
- Sutou, Y., Omori, T., Koeda, N., Kainuma, R. and Ishida, K. (2006). Effect of Grain Size & Texture on the Damping Properties of CuAlMn based SMA, *Mat. Sci & Eng. A* **438-440**. Pp. 743-746.
- Sutou, Y., Omori, T., Wang, J. J., Kainuma, R. and Ishida, K. (2004). Characteristics of CuAlMn based Shape Memory Alloys and their Applications, *Mat. Sci. & Eng.A* Vol. **378**, pp. 278-282.
- Sutou, Y., Omori, T., Yamauchi, K., Ono, N., Kainuma, R. and Ishida, K. (2005). Effect of Grain Size & Texture on Pseudoelasticity in CuAlMn based SMA Wire, *Acta. Materialia* **53**, pp. 4121-4133.
- Wilde, K., Gardoni, P. and Fujimo, Y. (2000). Base Isolation System with Shape Memory Alloy Device for Elevated Bridges, *Eng. Struct.* Vol. **22**, pp. 222-229.
- Wayman, C.M. and Duerig, T.W. (1990). An Introduction to Martensite and Shape Memory. Engineering Aspects of Shape Memory Alloys – Eds. Duerig, T. W., Melton, K. N., D. Stockel, Wayman, C. M., Published by Butterworth- Henemann, London, pp. 3-20.
- Zhang, Y., Camilleri, J. A. and Zhu, S. (2008). Mechanical Properties of Superelastic Cu-Al-Be Wires at Cold Temperatures for the Seismic Protection of Bridges, *Smart. Mater. & Struct.* Vol. **17**, 025008 (9pp).